ORIGINAL RESEARCH

Alterations in dysadherin expression and F-actin reorganization: a possible mechanism of hypericin-mediated photodynamic therapy in colon adenocarcinoma cells

Aysun Kılıç Süloğlu · Güldeniz Selmanoğlu · M. Turan Akay

Abstract Dysadherin is a recently found anti-adhesion molecule, therefore detection and down regulation of its expression is promising in cancer treatment. The up-regulation of dysadherin contributes to colon cancer recurrence and metastasis. Dysadherin also has connections with cytoskeletal proteins and it can cause alterations in the organisation of filamentous actin (F-actin) in metastatic cancers. In this study, hypericin (HYP)-mediated photodynamic therapy (PDT) was performed in two different grade colon adenocarcinoma cell lines HT-29 (Grade I) and Caco-2 (Grade II). Cells were treated with 0.04, 0.08 or 0.15 μM HYP concentrations and irradiated with (4 J/cm^2) fluorescent lamps. The effects of HYP was examined 16 and 24 h after the activation. We investigated for the first time the effect of HYP-mediated PDT on the expression of dysadherin and F-actin organisation. According to the results, HYP mediated PDT caused a decrease in gene expression and immunofluorescence staining of dysadherin and an increase in actin stress fibers and actin aggregates in HT-29 and Caco-2 cell lines. Besides, cytotoxicity, number of floating cells and apoptotic index changed depending on the cell type, HYP concentration and incubation time. We have demonstrated for the first time that dysadherin and F-actin could be target molecules for HYP-mediated PDT in HT-29 and Caco-2 colon cancer cell lines.

Introduction

Every year, colon cancer affects 1.23 million people and causes 608,000 deaths worldwide. It is the third most common malignant disease among men and the second among women (Ku et al. 2012). While surgical resection is the only known curative treatment, a significant number of patients still develop local recurrence and/or distant metastasis (Yang et al. 2012). Therefore, identification of factors that accurately predict the prognosis is essential. Although adjuvant chemotherapy or radiation therapy is needed after resection, unfortunately they are insufficient to eliminate the cancer tissue completely and to distinguish it from surrounding healthy tissues (Aoki et al. 2003; Salvador 2008). In this regard, it is essential to develop novel strategies and agents having improved pharmacologic profile and low toxicity without having drug resistance. Photodynamic therapy (PDT), a promising treatment for various types of cancer compared to conventional cancer therapies, is on the rise. PDT involves the administration of photosensitizing agent (PS), selective accumulation of PS in cancer cells, followed by irradiation with visible light,

A. Kılıç Süloğlu (✉) · G. Selmanoğlu · M. T. Akay
Department of Biology, Faculty of Science, Hacettepe University, Beytepe, 06800 Ankara, Turkey
e-mail: aykilic82@gmail.com

generation of reactive oxygen species (ROS), and PDT results in cell death (Sanovic et al. 2011). Possibility of repeated treatment, low systemic toxicity, selective accumulation without harmful side effects to healthy tissues, being applicable alone or in combination with currently used cancer therapies are remarkable advantages of PDT (Ackroyd et al. 2001; Allison and Sibata 2010). Several PS including HYP, are in advanced stages of clinical trials or in the approval phase for the treatment of several malignant and nonmalignant diseases. PDT has been approved in several countries for treatment of bladder, head and neck, lung, breast, esophageal, cervical and pancreatic cancers, but there are still loose ends in its clinical use and treatment of other cancer types, including colon cancer (Paszkoa et al. 2011; Yoo and Ha 2012).

In recent years, hypericin (HYP) has been the most frequently studied PS. HYP is a naturally occurring compound from *Hypericum perforatum* with approximately 595 nm wavelength light absorbance. HYP has advantages of minimal dark toxicity, high clearance from the body and high singlet oxygen production. Nevertheless, there are still question marks limiting its clinical use (Paszkoa et al. 2011). Depending on the HYP concentration, light dose, incubation time and cell origin, the type of cell death induced by PDT can be altered (Mikeš et al. 2007).

The fundamental goal of the cancer research is to identify molecules which are expressed only in cancer cells such as stomach, colon, pancreatic, and breast cancers rather than in normal cells. If these molecules have the potential to initiate tumor occurence or progression by chance, they become potential target molecules of novel treatment methods in order to prevent cancer (Nam et al. 2007). Dysadherin, a recently identified cell membrane glycoprotein, is expressed in a wide variety of cancer cells but relatively few in normal cells (Ino et al. 2002). It is estimated that dysadherin expression would be a good biological predictor for cell invasion and metastasis in human cancers (Hirohashi and Kanai 2003; Shimamura et al. 2004). It was reported that dysadherin expression has prognostic importance in advanced colorectal cancers (Batistatou et al. 2006). Dysadherin is also known as Fxyd domain containing ion transport regulator 5 (FXYD5). It interacts with Na–K ATPase, modulates its properties and down-regulates the expression of E-cadherin, therefore it is also called anti-adhesion molecule. The basis of human cancer morphogenesis is inactivation of cell adhesion. Recent studies have indicated that dysadherin expression increased in metastatic cancers. Therapies that are targeting down-regulation of dysaderin expression are expected (Nam et al. 2007).

Dysfunction of adhesion molecules or related cell cytoskeletal molecules is a significant step in development and progression of the majority of colon cancers (Buda and Pignatelli 2004). During the cancer invasion and metastasis, the cell motility is increased related with the cell cytoskeletal changes especially actin reorganisation (Wicki and Lehembre 2006). Moreover, dysadherin as a transmembrane protein has connections with cytoskeletal proteins and can cause alterations in the organisation of actin filaments with E-cadherin dependent or independent pathways in metastatic cancers (Nam et al. 2007). After PDT with different PS in various cancer cells, beside from morphological changes, actin cytoskeleton modifications are accompanied with cell adhesion changes (Di Venosa et al. 2012).

The aim of this study is to enlighten mechanisms underlying the effect of HYP-mediated PDT on anti-adhesive properties and cytoskeletal changes in colon cancer. In order to investigate the differences in response, different grade human colon adenocarcinoma cell lines, HT-29 and Caco-2 were used to compare dysadherin gene expression and actin filament organisation after PDT. The data generated in this study will also contribute to the clinical use of HYP in treatment of metastatic colon cancers.

Materials and methods

Cell lines and culture conditions

HT-29 (Grade I) and Caco-2 (Grade II) cells were obtained from HUKUK, Foot and Mouth Disease Institute (Ankara, Turkey). The cells were routinely maintained in Dulbecco's Modified Eagle Medium (HyClone Laboratories, Inc., Logan, UT, USA) supplemented with 10 % fetal bovine serum (PAA Laboratories, Linz, Austria) at 37 °C and 5 % CO_2 in a humidified incubator.

Photosensitizer and PDT procedure

Hypericin HPLC grade (AppliChem, Darmstadt, Germany), was prepared as a stock solution in DMSO

Scheme 1 Experimental groups and PDT procedure
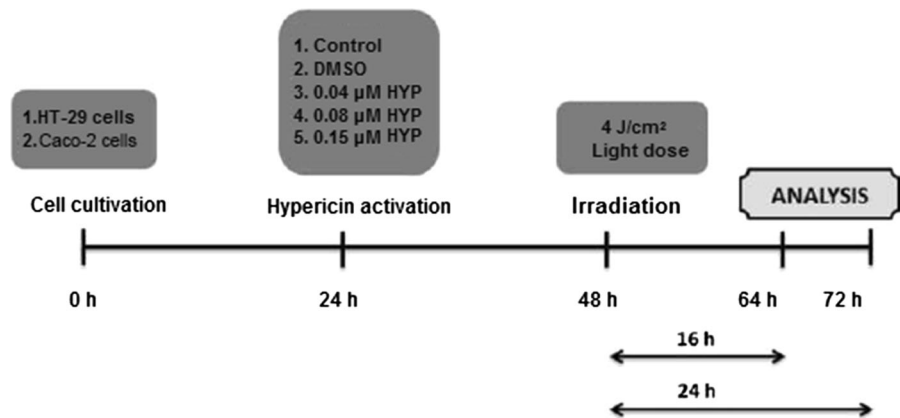
(final concentration is <0.1 %) and was diluted to particular working concentrations according to preliminary experiments. The cells were incubated with different concentrations of HYP (0.04, 0.08, 0.15 μM) in dark conditions for 24 h. Prior to irradiation, the medium containing HYP was replaced with fresh HYP-free DMEM without phenol red. Irradiation device consists of twelve L18W/830 fluorescent tubes (Osram, Berlin, Germany) with maximum emission in the range 530–620 nm, which covers HYP maximum absorbance. In order to avoid over heating eight fans were placed onto the device and temperature was measured throughout the irradiation. The light dose was measured with TES 1335 luxmeter (Rotronic, Taipei, Taiwan). HYP was activated by light at a total dose of 4 J/cm^2. The groups are control group (no HYP treatment but photoactivated), DMSO group (only DMSO treatment and photoactivated), HYP groups (0.04, 0.08, 0.15 μM HYP treatment and photoactivated). A dark control group treated with 0.15 μM HYP without irradiation was also included. Analysis were performed 16 and 24 h after irradiation (Scheme 1).

Cell number and floating cell quantification

Cells were seeded in six-well plates with the same initial cell number (60×10^4) for control and HYP treatment groups in order to count cell number after PDT. After staining with 0.5 % trypan blue, viability was evaluated in a Bürker chamber by using light microscopy. The number of floating cells in the supernatant was presented in order to show the increase in dead cells due to HYP cytotoxicity.

MTT assay

Cells were suspended in a complete medium (HyClone Laboratories, Inc. Logan, UT, USA), seeded into 96-well microculture plates, and incubated for 24 h. After 16 and 24 h from HYP activation, 3-(4,5-dimethylthiazol-2-yl)-2,5-diphenyl tetrazolium bromide (MTT, Sigma, St. Louis, MO, USA) was added. After incubation for 4 h, isopropanol was added and optical density at 570 nm was recorded with a microplate reader (Bio Tek Instruments Inc., Winooski, VT, USA). Experiments have been triplicated and surviving cell % was defined as the treatment group/control group (control group assumed as 100 % survival).

Analysis of hypericin content

After HYP activation floating and adherent cells were harvested together, washed and resuspended in PBS, and the fluorescence of HYP was analyzed using flow cytometer (EPICS XL-MCL Beckman Coulter, Brea, CA, USA). In order to measure the intensity of HYP fluorescence in the cells CellQuestPro software was used. HYP content was evaluated as mean fluorescence intensity (MFI) and as the ratio of MFI in treatment/control group (relative fluorescence intensity, RFI) (Jendzelovsky et al. 2009).

Quantification of apoptosis index by DAPI staining

Cells were stained with 4,6-diamidino-2-phenylindole (DAPI, Hyclone) and scored as apoptotic according to condensation and fragmentation of nuclear DNA by nuclear morphological analysis. At least 200 cells were

counted in each sample and the number of apoptotic and normal nuclei were determined under fluorescence microscope (Olympus IX71, Tokyo, Japan). The apoptotic index was calculated as apoptotic/total number of cells × 100.

Table 1 Floating cell number ($\times 10^4$) in HT-29 and Caco-2 cell populations

	Incubation time (h)	
	16 h	24 h
HT-29		
Control	2.0 ± 0.01	4.0 ± 0.2
0.04 μM HYP	5.0 ± 0.05[b]	8.1 ± 0.1[a]
0.08 μM HYP	9.5 ± 0.11[a]	8.9 ± 0.37[a]
0.15 μM HYP	12 ± 0.03[a]	9.8 ± 0.06[a]
Caco-2		
Control	0.28 ± 0.002	0.55 ± 0.009
0.04 μM HYP	0.83 ± 0.01[b]	0.22 ± 0.03[b]
0.08 μM HYP	1.30 ± 0.007[a]	0.33 ± 0.0012[b]
0.15 μM HYP	2.36 ± 0.01[a]	1.46 ± 0.06[a]

The cells were treated with hypericin (0.04, 0.08 and 0.15 μM HYP), irradiated with 4 J/cm^2 and harvested 16 or 24 h after PDT. The results (mean ± SE) of three independent experiments are shown

[a] Statistically significant from control group ($P \le 0.05$)

[b] Statistically significant from 0.15 μM HYP group ($P \le 0.05$)

Immunofluorescent staining (IF) of F-actin and dysadherin

Cells were incubated and fixed in 4 % paraformaldehyde for 10 min, incubated with 0.1 % TritonX-100, washed in PBS, blocked for 30 min in 2 % goat serum (Santa Cruz Biotechnology, Inc., Santa Cruz, CA, USA). Then, the cells were incubated with anti-dysadherin antibody (1:50 diluted) (Santa Cruz Biotechnology, Inc., Santa Cruz, CA, USA) at 4 °C overnight in a moist chamber, followed by Texas red labeled secondary antibody incubation (Santa Cruz Biotechology, Inc., Santa Cruz, CA, USA) for 60 min. Alexa fluoro 488-conjugated phalloidin (Invitrogen, CA, Santa Cruz, CA, USA) was applied directly to visualize F-actin. The samples were then mounted with mounting medium and examined by fluorescence microscope. The experiments were performed in triplicate.

Quantification of dysadherin expression with reverse transcriptase polymerase chain reaction (RT-PCR)

Total RNA was extracted from HT-29 and Caco-2 cells with Qiagen Rneasy Mini Kit (Valencia, CA, USA) and was quantified in NanoDrop 2000c (Thermoscientific, West Palm Beach, FL, USA). The total RNA was reverse transcribed with using an oligo(dT)
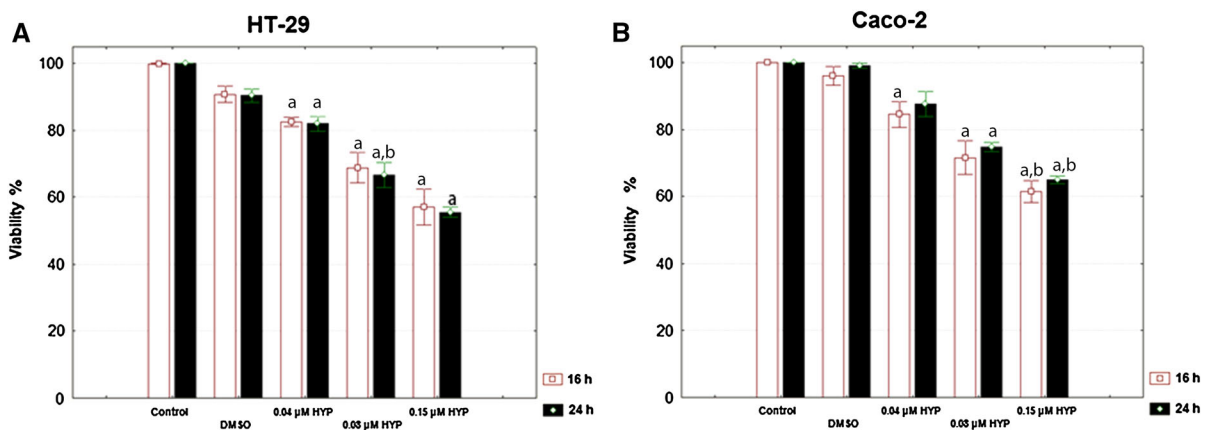

Fig. 1 HYP photocytotoxicity (MTT test) in (**A**) HT-29 and (**B**) Caco-2 cells 16 and 24 h after PDT. The cells were treated with HYP (0.04, 0.08 and 0.15 μM HYP), irradiated with 4 J/cm^2 and harvested 16 or 24 h after PDT. The results

(mean ± SE) of three independent experiments are shown as % of the untreated control. *a* statistically significant from control group, *b* statistically significant from 0.04 μM HYP group ($P \le 0.05$)
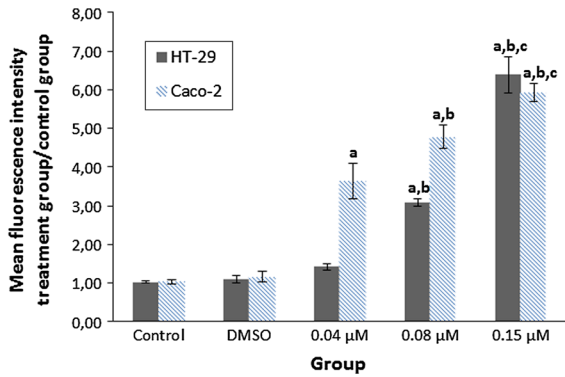
Fig. 2 0.04, 0.08, 0.15 μM HYP accumulation in HT-29 and Caco-2 cells measured with a flow cytometer 24 h after HYP-mediated PDT, expressed as the ratio of mean fluorescence intensity of treatment/control group. *a* statistically significant from control group, *b* statistically significant from 0.04 μM HYP group ($P \leq 0.05$). *c* statistically significant from 0.08 μM HYP group ($P \leq 0.05$)

primer Invitrogen SuperScript III First Strand Synthesis System for RT-PCR kit. First strand cDNA was synthesized from 0.5 mg of RNA. Semiquantitative RT-PCR was performed and the template cDNA was amplified by the use of Go Taq Flexi DNA polymerase (Promega, Madison, WI, USA). For standardization of the amount of template cDNA, expression of cyclophilin A (a house keeping gene) was quantified in each sample. The primer sets for amplification of dysadherin and cylophilin A cDNA were as follows: dysadherin, 5′-TCCCACTGATGACACCACGA-3′ (forward primer), 5′ACTTGCCACTGGTGAGGATG AT-3′ (reverse primer), cylophilin A, 5′-AGGTCCCCA AAGACAGCAGAA-3′ (forward primer), 5′TGTCC ACAGTCAGCAATGGT-3′ (reverse primer) PCR products were subjected to agarose gel (2 %) electrophoresis and visualized by ethidium bromide staining. The gel was viewed and captured as a digital image by
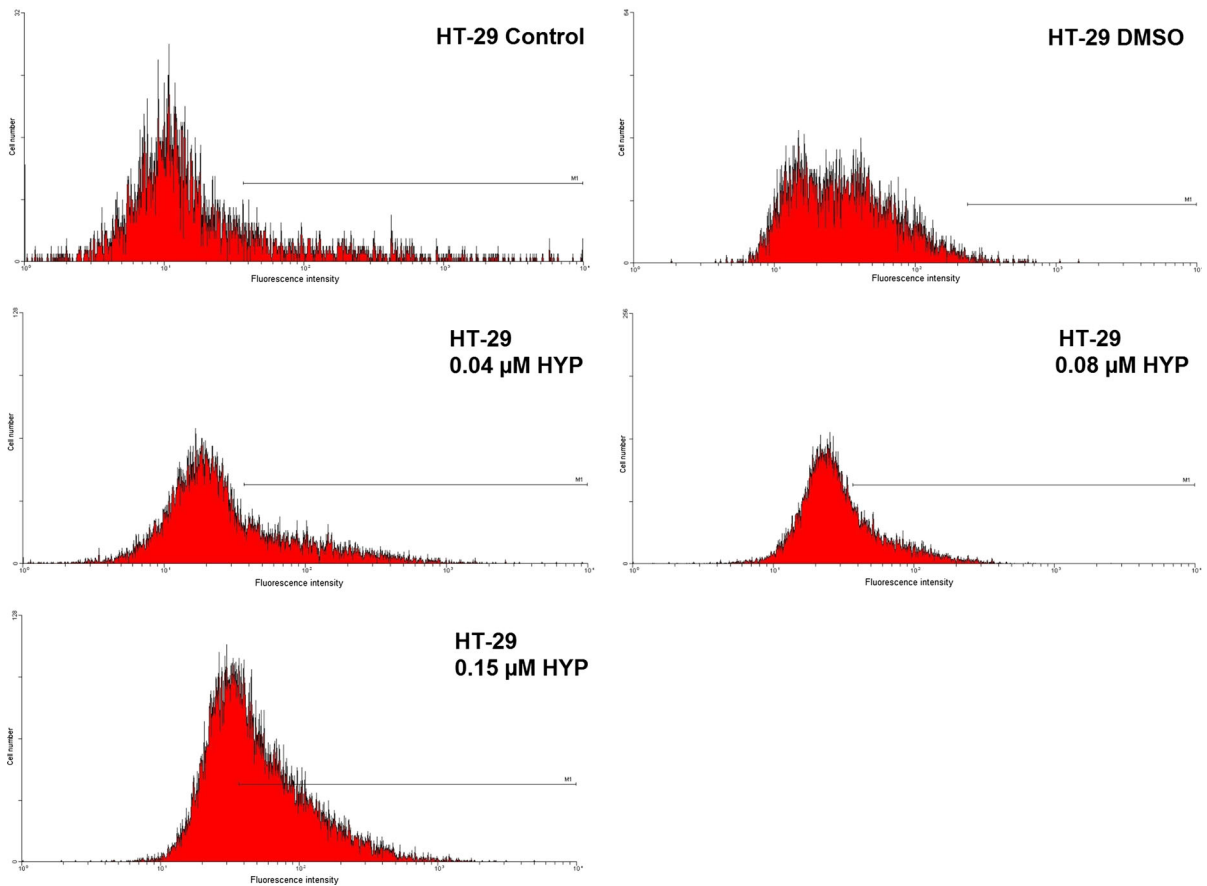

Fig. 3 Histograms of HYP fluorescence intensity using flow cytometer in HT-29 cells 24 h after PDT
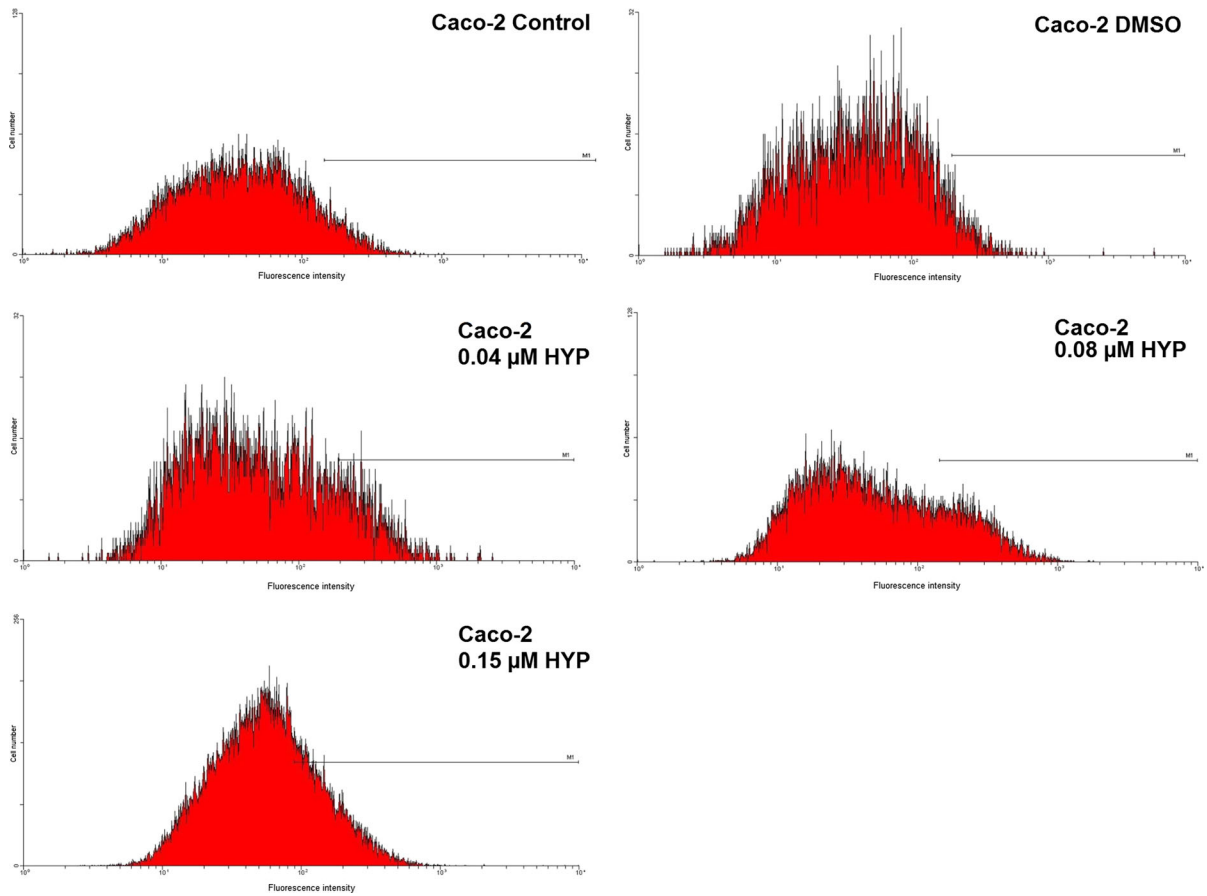
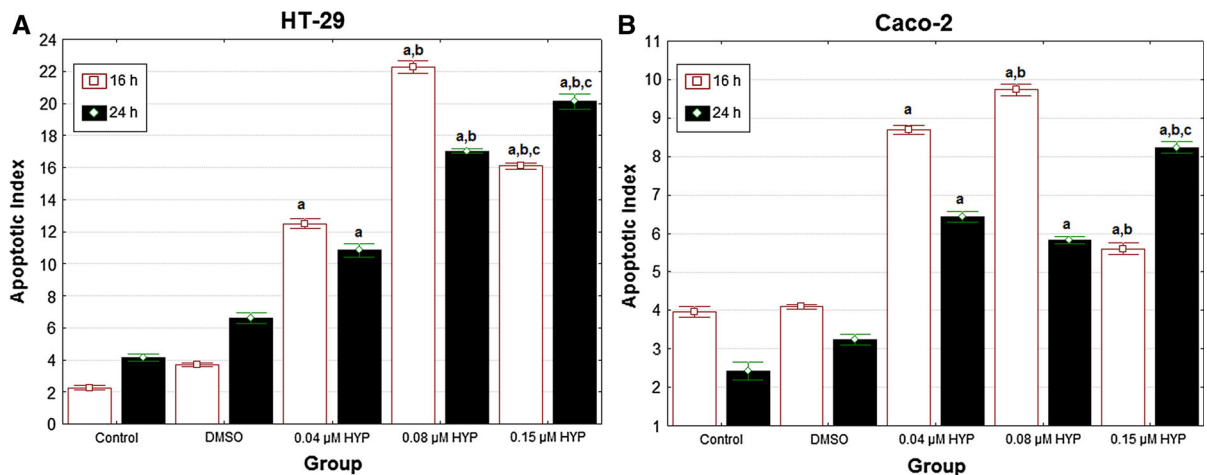**Fig. 4** Histograms of HYP fluorescence intensity using flow cytometer in Caco-2 cells 24 h after PDT

Fig. 5 Apoptotic cell % of treatment groups compared to control group (apoptotic index) in (**A**) HT-29 and (**B**) Caco-2 cells is presented. The cells were treated with HYP (0.04, 0.08 and 0.15 μM HYP), irradiated with 4 J/cm^2 and harvested 16 or 24 h after PDT. *a* statistically significant from control group ($P \leq 0.001$), *b* statistically significant from 0.04 μM HYP group, *c* statistically significant from 0.08 μM HYP group ($P \leq 0.05$)

the Syngene Gene Genius and quantified by Gene Tools Analysis Software 3.02.00 (Syngene, Frederick, MD, USA). The experiments were performed in triplicate and results were given as the relative dysadherin expression level (dysadherin/cyclophilin A expression).

Western blot analysis

Cells were lysed on ice for 30 min with lysis buffer (25 mM TrisHCl pH 7.6, 150 mM NaCl, 1 % NP-40, 1 % sodium deoxycolate, 0.1 % SDS) (Pierce Biotechnology 89901, Rockford, IL, USA). The supernatant
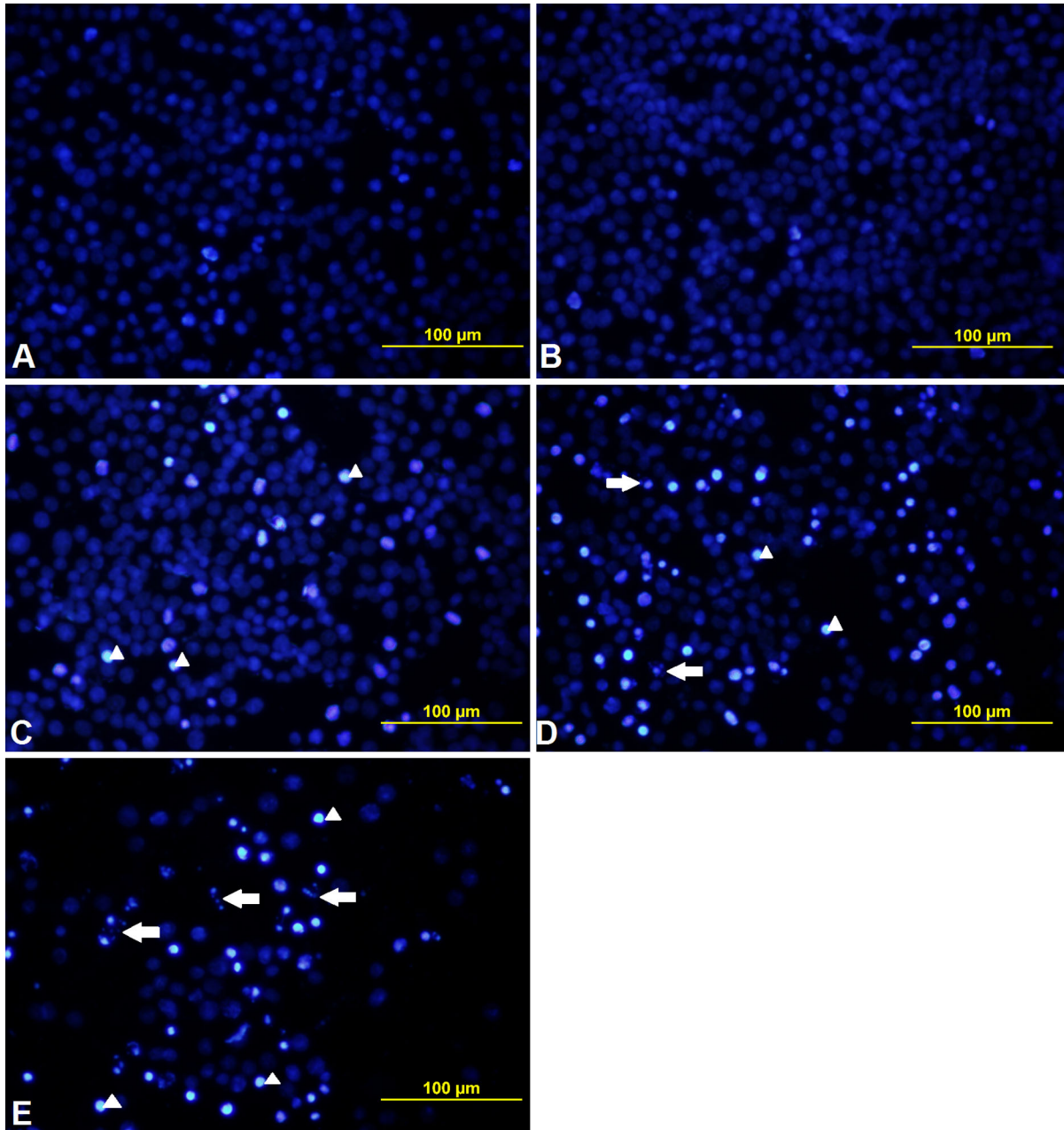

Fig. 6 HT-29 cells were incubated with different concentrations of HYP and 16 h after PDT HYP-induced apoptosis was determined by DAPI staining using fluorescence microscopy. Control group (**A**), DMSO (**B**), HYP treatment groups 0.04 μM (**C**), 0.08 μM (**D**) and 0.15 μM HYP (**E**). *arrow head* nuclear condensation, *arrow* nuclear fragmentation

was collected after centrifugation (15,000 rpm for 30 min) and the amount of total protein was measured using BCA kit (Pierce Biotechnology 23227, Rockford, IL, USA). Samples of 30 μg protein per lane were separated by SDS PAGE (12.5 %) and then transferred

to a nitrocellulose membrane. The membrane was incubated with a monoclonal anti-dysadherin antibody (Santa Cruz Biotechnology sc-98246, Santa Crus, CA, USA). Blots were developed with chemiluminescence reagents (BM chemiluminescence blotting substrates;
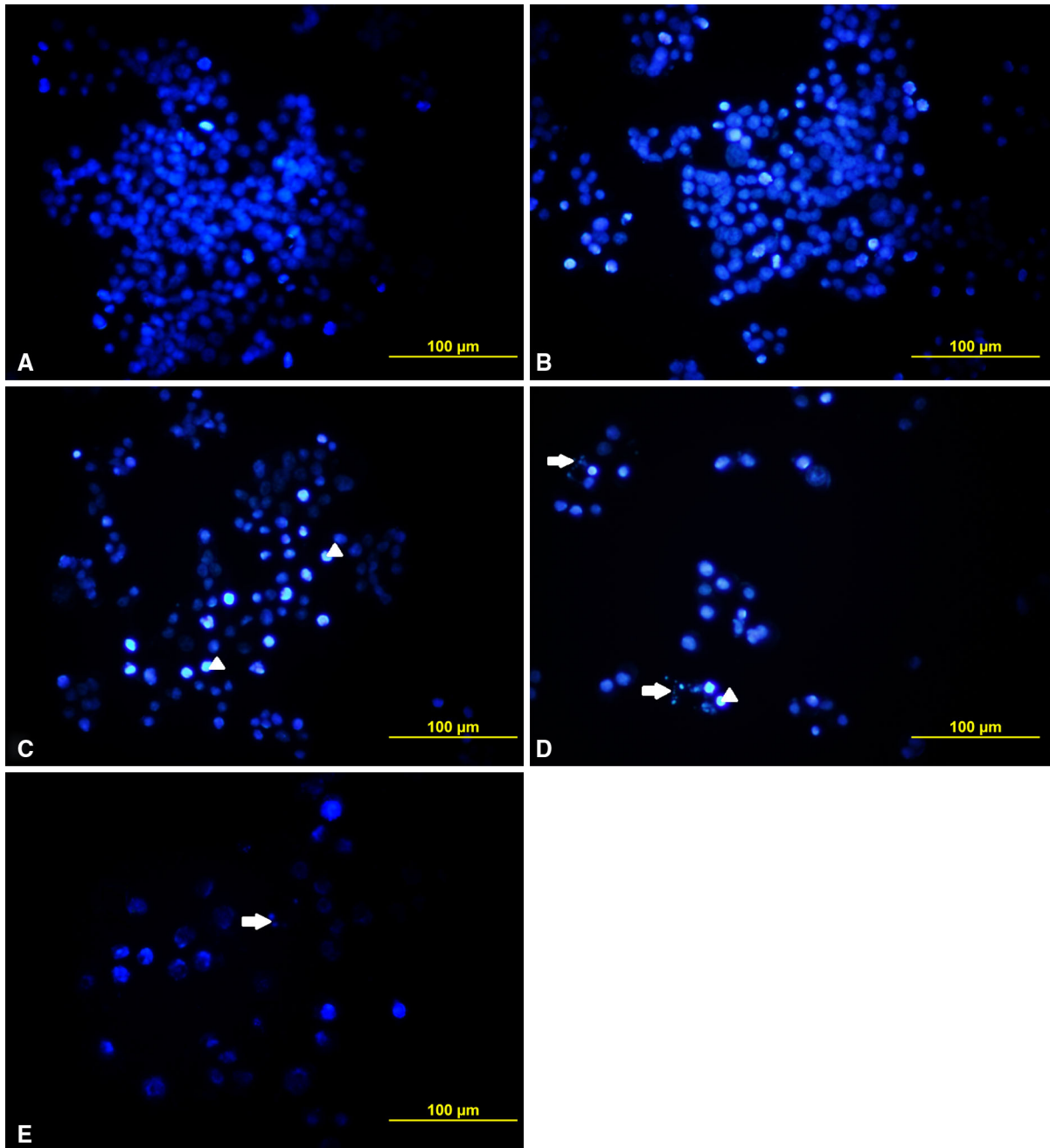

Fig. 7 HT-29 cells were incubated with different concentrations of HYP and 24 h after PDT HYP-induced apoptosis was determined by DAPI staining using fluorescence microscopy. Control group (**A**), DMSO (**B**), HYP treatment groups 0.04 μM (**C**), 0.08 μM (**D**) and 0.15 μM HYP (**E**). *arrow head* nuclear condensation, *arrow* nuclear fragmentation

Boehringer Mannheim, Roche Molecular Biochemical, Mannhaim, Germany) and immunoreactive bands were detected by autoradiography. Jurkat whole cell lysate (Santa Cruz Biotechnology sc-2204, Santa Cruz, CA, USA) was used as a positive control.

Statistical analysis

A statistical analysis was performed using the STAT-ISTICA program for Windows. Data were expressed as mean ± standard error (SE) and statistical
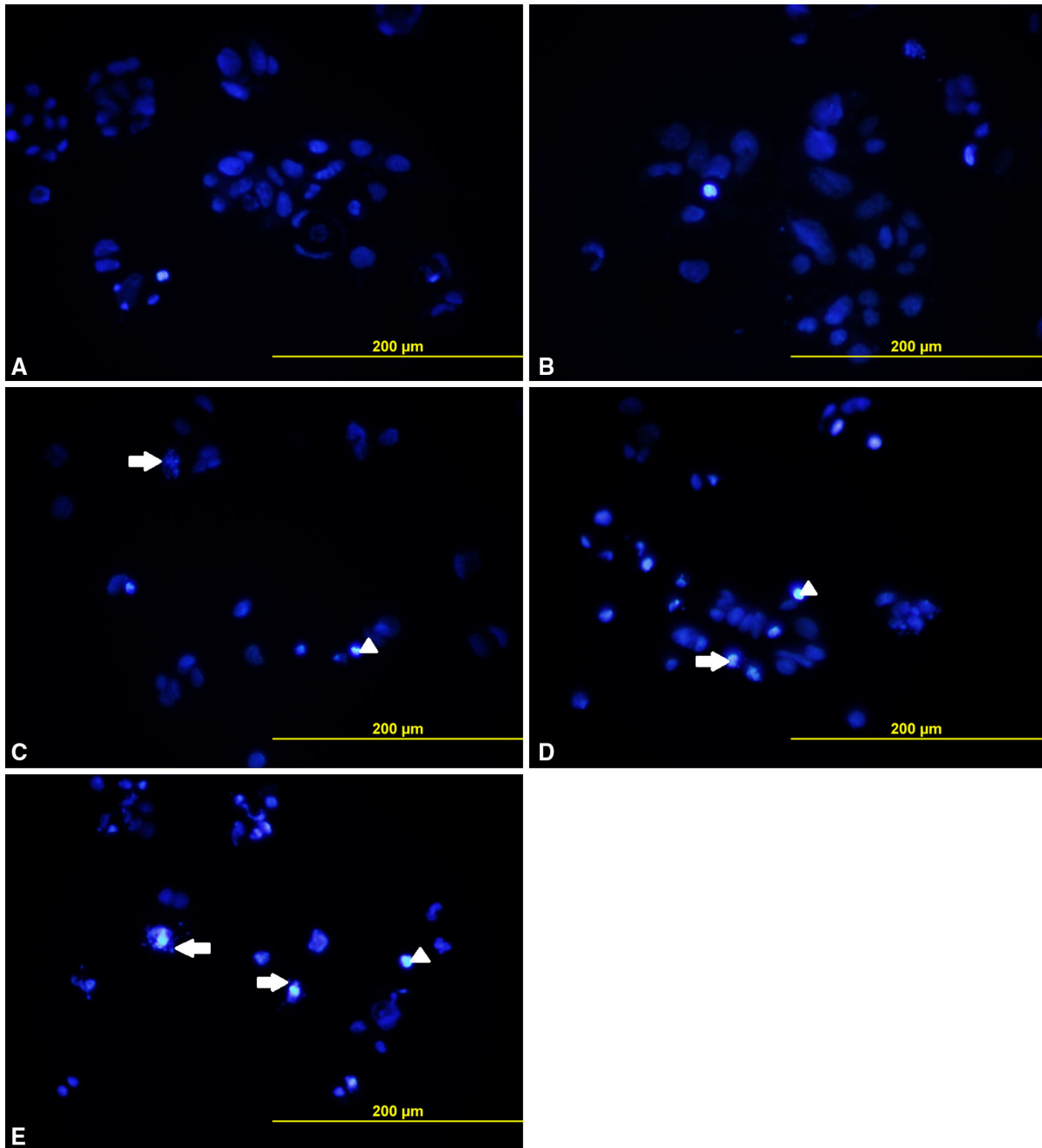

Fig. 8 Caco-2 cells were incubated with different concentrations of HYP and 16 h after PDT HYP-induced apoptosis was determined by DAPI staining using fluorescence microscopy. Control group (**A**), DMSO (**B**), HYP treatment groups 0.04 μM (**C**), 0.08 μM (**D**) and 0.15 μM HYP (**E**). *arrow head* nuclear condensation, *arrow* nuclear fragmentation

significance was assigned at the $P \leq 0.05$ level. The homogeneity of variance and normal distribution between groups were evaluated by General Linear Model procedure and Kolmogorov–Smirnov

nonparametric test. Data were analysed using one-way ANOVA with Tukey's post hoc test. Factorial ANOVA was used to analyse differences depending on both incubation time and HYP concentration.
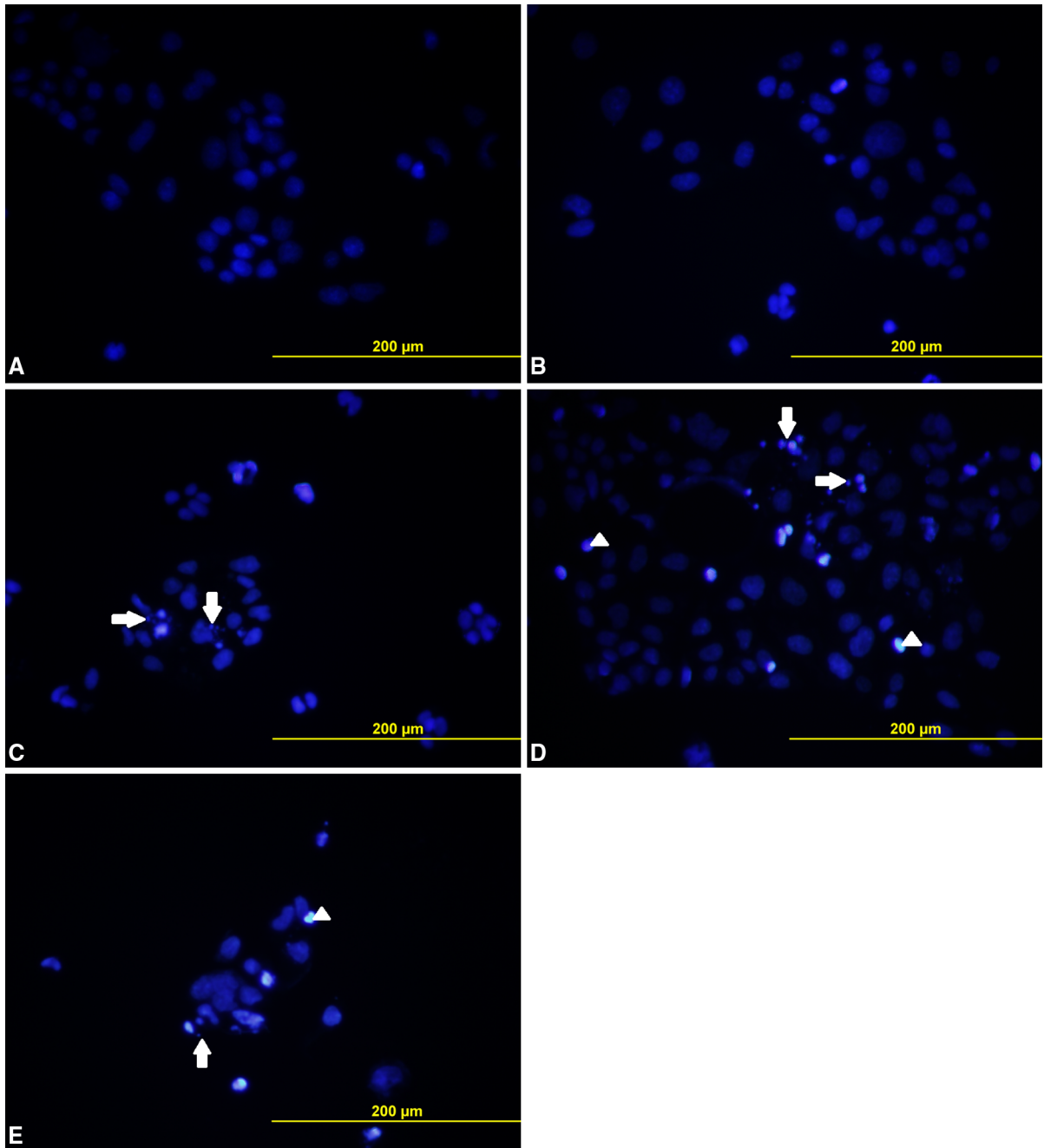

Fig. 9 Caco-2 cells were incubated with different concentrations of HYP and 24 h after PDT HYP-induced apoptosis was determined by DAPI staining using fluorescence microscopy. Control group (**A**), DMSO (**B**), HYP treatment groups 0.04 μM (**C**), 0.08 μM (**D**) and 0.15 μM HYP (**E**). *arrow head* nuclear condensation, *arrow* nuclear fragmentation

Results and discussion

HT-29 and Caco-2 cells differentiate spontaneously and form typical intestine villus structured colon cancer cells which express specific intestine enzymes (Mitchell and Ball 2004). Previously, HYP-mediated PDT in HT-29 cells was investigated. On the other hand, there are no reports about the response in Caco-2 cells and the possible action mechanism of HYP on anti-adhesion molecule dysadherin and cell cytoskeletal element F-actin after PDT. In this study, after HYP-mediated PDT, HT-29 and Caco-2 colon adenocarcinoma cells were compared for cytotoxicity, types of cell death, immunostaining of dysadherin and F-actin and also gene expression of dysadherin for two incubation times.

According to the results, no significant differences were observed between control, DMSO and dark control groups. We observed that after HYP activation, number of the floating cells were markedly elevated. In HT-29 cells, the increase in floating cells were significant in HYP groups compared to the control group for both incubation times. Our results are consistent with the work of Mikeš et al. (2007) in which floating cells were increased depending on the HYP concentration and incubation time in HT-29 cells. In Caco-2 cells, increase in the number of floating cells was statistically significant in 0.04, 0.08 and 0.15 µM HYP groups compared to control group after 16 h after PDT (Table 1). 24 h after PDT the increase of floating cells was significant only in the 0.15 µM HYP group compared to control group.

It is known that phototoxicity of HYP is closely associated with the cell type. In various cancer cells after HYP-mediated PDT, cell death induction was related with mitochondrial membrane potential and
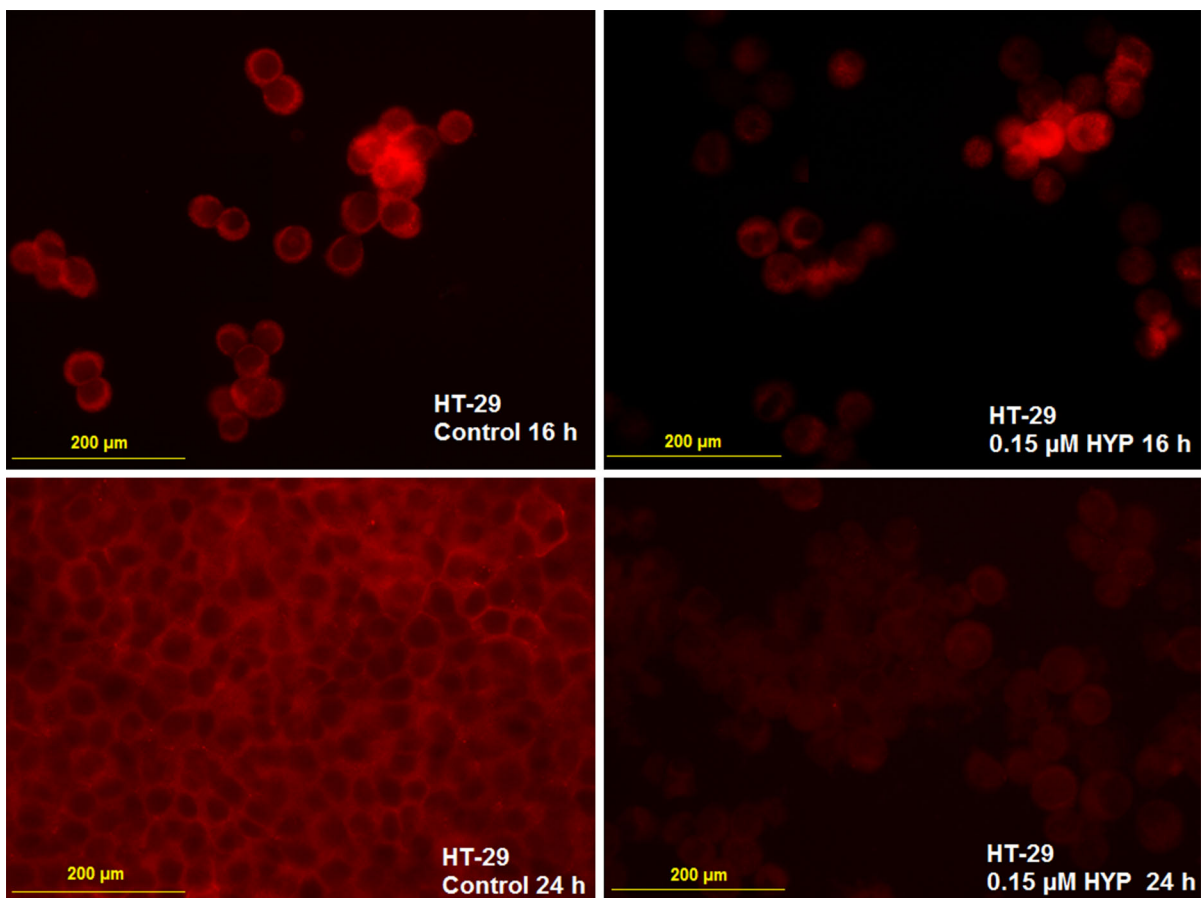

Fig. 10 Immunofluorescence staining of dysadherin (cell membrane, *red color*) in HT-29 cells 16 and 24 h after PDT. Magnification ×400. (Color figure online)

mitochondrial enzyme alterations, resulted in hydroxyl radical formation and lipid peroxidation (Theodossiou et al. 2009). It was reported that HYP is accumulated mostly in mitochondria, endoplasmic reticulum, Golgi appartus and slightly in lysosomal membrane (Galanou et al. 2008). MTT assay (based on mitochondrial activity) and neutral red assay (based on lysosomal activity, data not shown) were performed in order to determine cytotoxicity. According to the results, HYP was found to be more cytotoxic in MTT assay due to the primarily affected mitochondria. HYP concentration dependent phototoxicity was seen in both HT-29 and Caco-2 cells (Fig. 1). Considerable differences in MTT assay between HT-29 and Caco-2 cells were observed after PDT. In the same PDT conditions, cytotoxicity in Caco-2 cells was lower than in HT-29 cells. Cytotoxicity decreased in Caco-2 cells and increased in HT-29 cells 24 h after PDT.

According to Dahl et al. (2006), cytotoxicity can be graded as follows, non-toxic (>90 % cell viability), slight toxic (60–90 % cell viability), moderately toxic (30–59 % cell viability), and toxic (<30 % cell viability). Control and DMSO groups were graded as non-toxic, 0.04 and 0.08 μM HYP concentrations were slightly toxic in HT-29 and Caco-2 cells for both incubation times. 0.15 μM HYP concentration was graded as moderately toxic in HT-29 and slightly toxic in Caco-2 cells. For both of the cells, the viability increased 48 h after irradiation (data not shown).

Without irradiation HYP does not emit fluorescence light, but after activation with the appropriate wavelength light, fluorescence light emission starts. The relative intracellular HYP accumulation can be evaluated by measuring fluorescence intensity in flow cytometer (Yamazaki et al. 1993). In this study, the HYP content increased depending on the
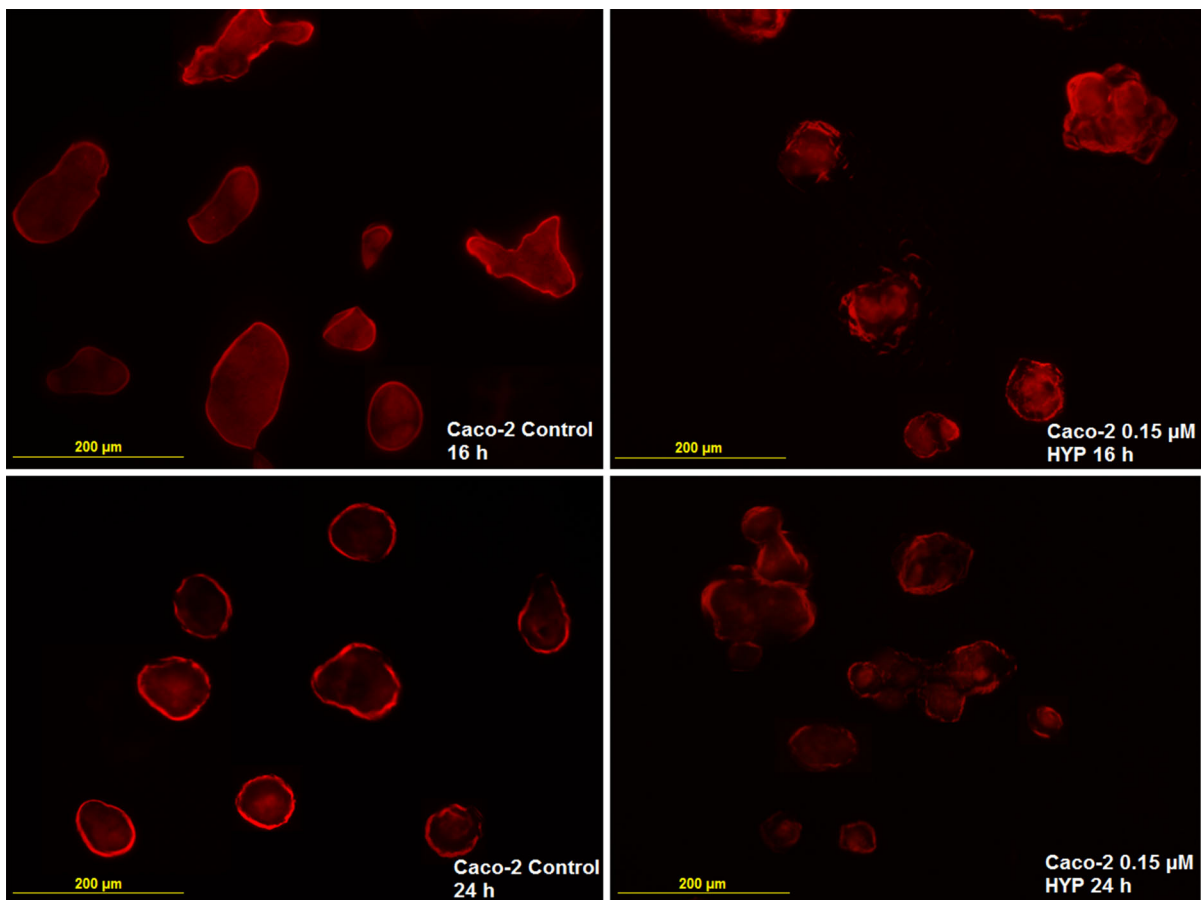

Fig. 11 Immunofluorescence staining of dysadherin (cell membrane, *red color*) in Caco-2 cells 16 and 24 h after PDT. Magnification ×400. (Color figure online)

accumulation in HT-29 and Caco-2 cells (Fig. 2). The relative fluorescence intensity rose in treatment groups indicating the increase in intracellular HYP accumulation. The fluorescence intensity is also presented in histograms (Figs. 3, 4). In the only study conducted with Caco-2 cells, HYP and protohypericin were accumulated 4–8 % in the cell and membranes 3 h after activation (Kamuhabwa et al. 1999). In this study, it was observed that cellular HYP uptake was high in Caco-2 cells for 0.04 and 0.08 μM HYP concentrations but, in HT-29 cells HYP accumulation was higher in the 0.15 μM HYP treatment group.

The induction of apoptosis after HYP-mediated PDT in HT-29 and Caco-2 cells is presented in Fig. 5. Apoptotic index increased depending on HYP concentration both in HT-29 and Caco-2 cells. 24 h after PDT apoptotic index was higher than for 16 h incubation for 0.15 μM HYP concentration in both cell types but not

for low HYP concentrations. Cyclooxygenase-2 (COX2) has a significant role in colon cancer progression with its anti-apoptotic effect, promoting invasion and angiogenesis. While HT-29 cells have high COX-2 expression, Caco-2 cells have low COX-2 expression level (Lev-Ari et al. 2005). 16 h after PDT apoptotic cell % was higher in low HYP concentration group in Caco-2 cells compared to HT-29 cells possibly due to low COX-2 expression. It was reported that HYP-mediated PDT of human cancer cells leads to up-regulation of the inducible COX-2 (Hendrickx et al. 2003). The cytotoxic effect of HYP started to decrease and possibly PDT induced resistance against apoptosis in Caco-2 cells 24 h after PDT.

DAPI IF stainings are presented in Figs. 6, 7 for HT-29 cells, and Figs. 8, 9 for Caco-2 cells. At low HYP concentration (0.04 μM) early apoptotic cells characterised by nuclear condensations were seen
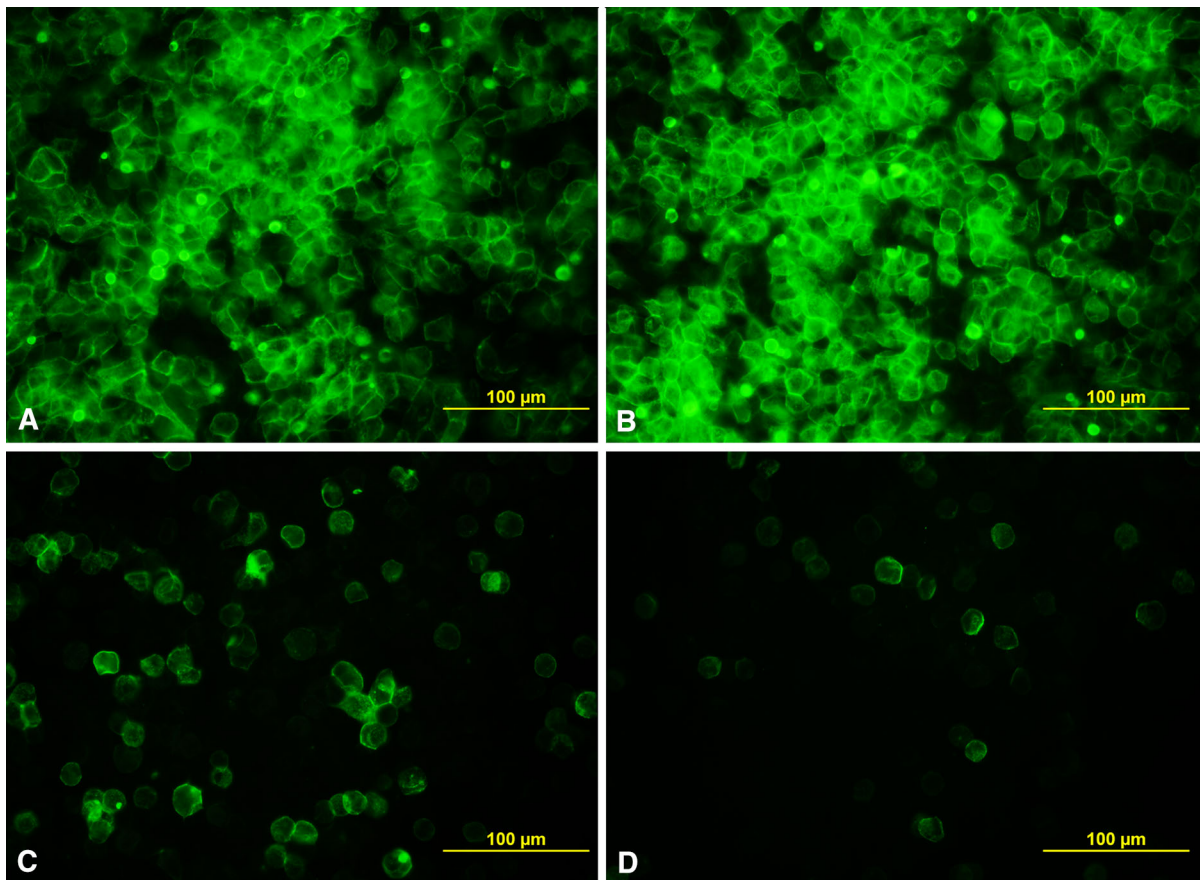

Fig. 12 Immunofluorescence staining of F-actin (*green*) in HT-29 cells. The cells were untreated (**A**) or treated with HYP 0.04 μM (**B**), 0.08 μM (**C**) and 0.15 μM HYP (**D**), irradiated with 4 J/cm^2 and harvested 16 h after PDT. *arrow head* actin aggregates, *arrow* actin stress fibers. (Color figure online)

more frequently. In the 0.08 and 0.15 μM HYP groups, number of late apoptotic cells having fragmented nuclei and apoptotic bodies increased.

Escaping from apoptosis and continuous proliferation are characteristic properties of cancer cells. New molecules which are targeting apoptosis by intrinsic or extrinsic pathways, have a significant role in cancer treatment (Ashkenazi 2002). Both HT-29 and Caco-2 cells are p53 mutant which contributes colon cancer metastasis and aggressiveness. In recent years, p63 and p73 proteins were found to belong to the p53 protein family. Caco-2 cells are p53 mutant but they have wild type of p63 and p73 genes, therefore these genes are possibly related to the apoptosis seen in these cells (Ray et al. 2011). But both cells also express anti-apoptotic Bcl-2 which is inhibiting cytochrome-c release and caspase-3 activation. This may

cause developing resistance against apoptosis seen in the 0.15 μM HYP group, and finally cell death shifts to necrosis (Reed 1998).

FXYD5, is one of the FXYD protein family members known as dysadherin or anti-adhesion molecule. Dysadherin interacts with and modulates the activity of the Na–K ATPase, contributes to cell adhesion, motility and actin organisation. The subdomains of Na–K ATPase interacts with cytoskeletal proteins by phosphoinositide 3-kinase and causes reorganisation and lamellipodia formation (Kaplan 2005). The role of dysadherin in cell–cell interaction and cell adhesion is related to its long extracellular domain which is heavily and heterogeneously glycosylated (Nam et al. 2007). Cell motility as one of the phenotypes observed in vitro, can reflect the in vivo metastatic potential of the cell. Furthermore, it was
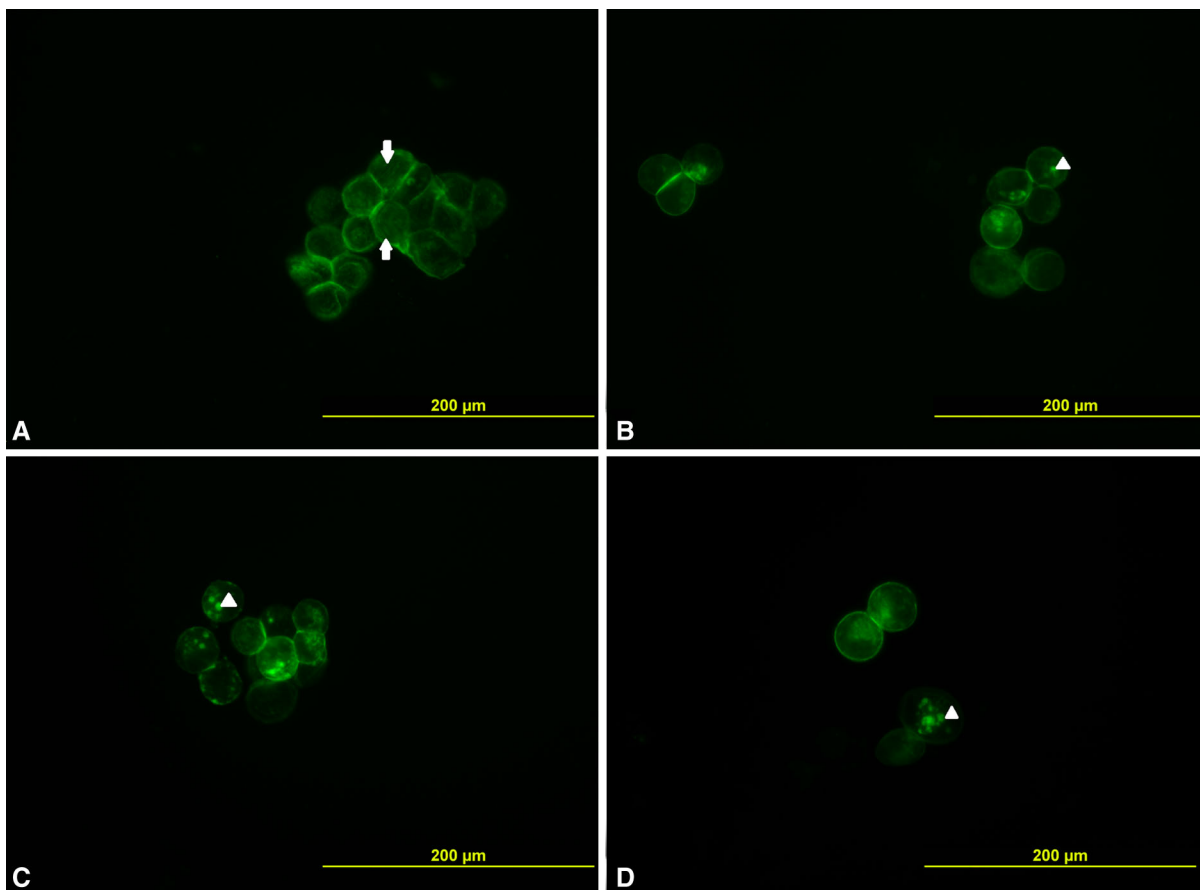

Fig. 13 Immunofluorescence staining of F-actin (*green*) in HT-29 cells. The cells were untreated (**A**) or treated with HYP 0.04 μM (**B**), 0.08 μM (**C**) and 0.15 μM HYP (**D**), irradiated with 4 J/cm^2 and harvested 24 h after PDT. *arrow head* actin aggregates, *arrow* actin stress fibers. (Color figure online)

shown that cancer cells which were over expressing dysadherin, have increased metastatic potential (Shi-mamura et al. 2004).

In this study, dysadherin IF staining was expressed at the cell membrane in control groups after 16 and 24 h activation in HT-29 and Caco-2 cells. In the HYP treatment groups dysadherin IF staining intensity decreased depending on HYP concentration for both cells (Figs. 10, 11). Submembranous cortical actin layer and regular actin stress fibers were observed in the cytoplasm of control groups (Figs. 12A–15A). For HT-29 cells 24 h after PDT and for Caco-2 cells 16 h after PDT cortical actin layer staining and dysadherin staining decreased. Actin aggregates were observed 24 h after HYP-mediated PDT in HT-29 and Caco-2 cell cytoplasm (Figs. 12–15).

The results of molecular analysis for dysadherin expression were in accordance with IF staining

results. Total RNA was isolated and analyzed by RT-PCR for the expression of dysadherin and cylophillin A. Cylophillin A expression was similar in untreated and HYP treated cells. The expression level of dysadherin decreased statistically in HYP treated groups of HT-29 cells 24 h after PDT, especially in the 0.15 μM HYP group (Fig. 16). In Caco-2 cells, the only affected group for dysadherin expression was the 0.15 μM HYP group after 16 h from PDT (Fig. 16). These results showed that HYP-mediated PDT affected dysadherin expression at RNA level. Results were supported with the western blot analysis showing the alterations also at protein level (Figs. 17, 18).

Dysadherin positive cell populations have high cell proliferation rates and show anti-apoptotic properties (Park et al. 2011). Parallel to their findings, in this study we observed that while dysadherin expression
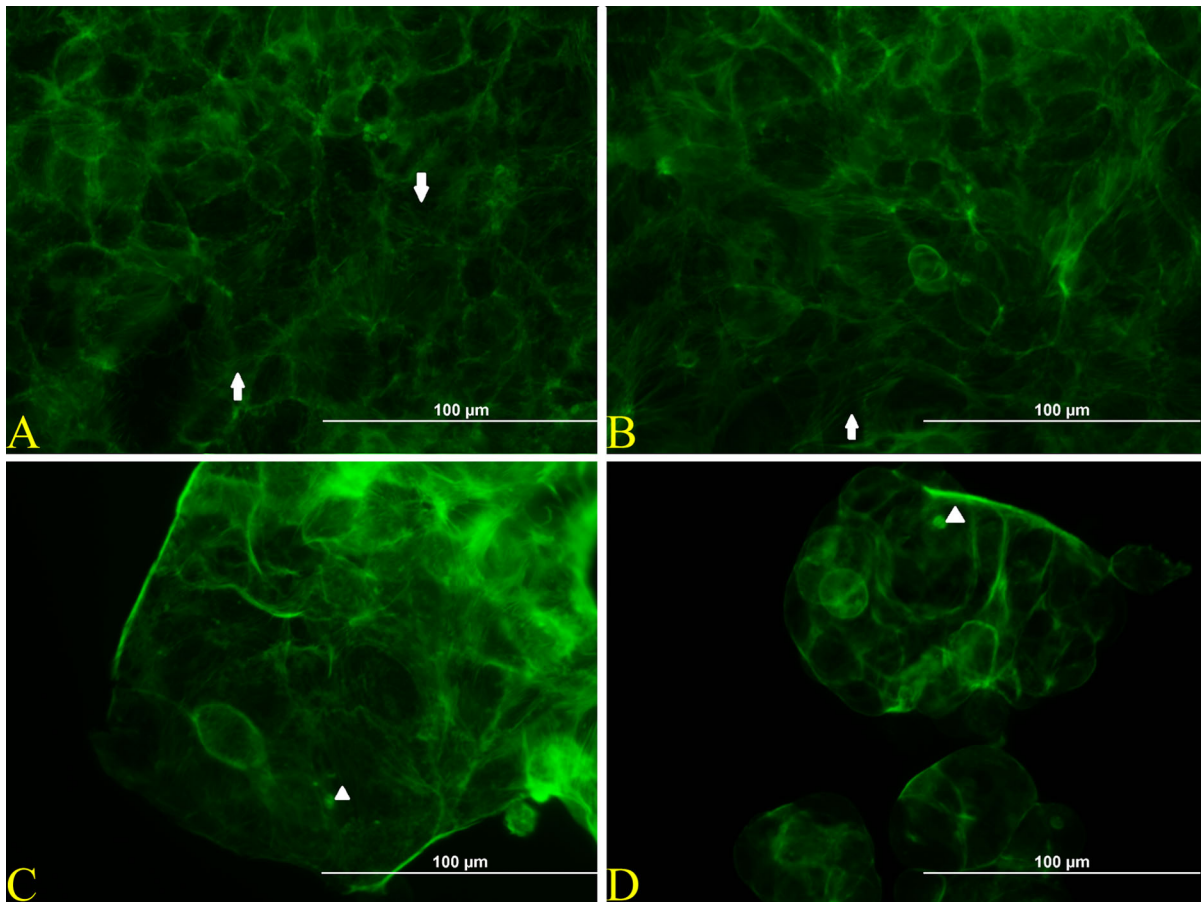

Fig. 14 Immunofluorescence staining of F-actin (*green*) in Caco-2 cells. The cells were untreated (**A**) or treated with HYP 0.04 μM (**B**), 0.08 μM (**C**) and 0.15 μM HYP (**D**), irradiated with 4 J/cm² and harvested 16 h after PDT. *arrow head* actin aggregates, *arrow* actin stress fibers. (Color figure online)

decreased, apoptosis increased in HT-29 and Caco-2 cells depending on the HYP concentration.

Hyperforin is another derivative of *Hypericum perforatum* plant. It was shown that hyperforin inhibits several enzymes which are also inhibited by HYP and affect the activity of several ion channels (Šemelakova et al. 2012). We suggest that HYP could affect Na–K ATPase due to the decreased expression of dysadherin which is one of the regulators of this pump.

Cancer cells can spontaneously migrate into the tissue during invasion and metastasis, therefore it is crucial to control cell migration for developing new cancer treatment strategies. Actin cytoskeleton, and most of its regulatory proteins are necessary for cell migration (Coates et al. 1992). In epithelial cells, there are strong cell–cell connections and the subcortical actin skeleton is localized under the cell membrane.

The alterations in the amount of F-actin in any part of the cell reflect the balance between actin polymerization and F-actin depolymerization. Serial increases and decreases in F-actin content can cause change in distribution of F-actin from diffuse to focal (Coates et al. 1992). During cell migration, actin cytoskeleton is reorganized. The inhibition of this dynamic process contributes to decrease in the cell motility which is a very desirable outcome for cancer treatment (Yamazaki et al. 2005). In this study we demonstrated that high HYP concentrations affected cytoplasmic stress fibers in HT-29 and Caco-2 cells. It was reported that in HT-29 cells, actin disrupting agents caused more adherent cancer cells and alterations were observed in metastasis in vivo (Korb et al. 2004). In a study conducted with pancreatic cancer cells, alterations in dysadherin expression affected cell morphology, actin
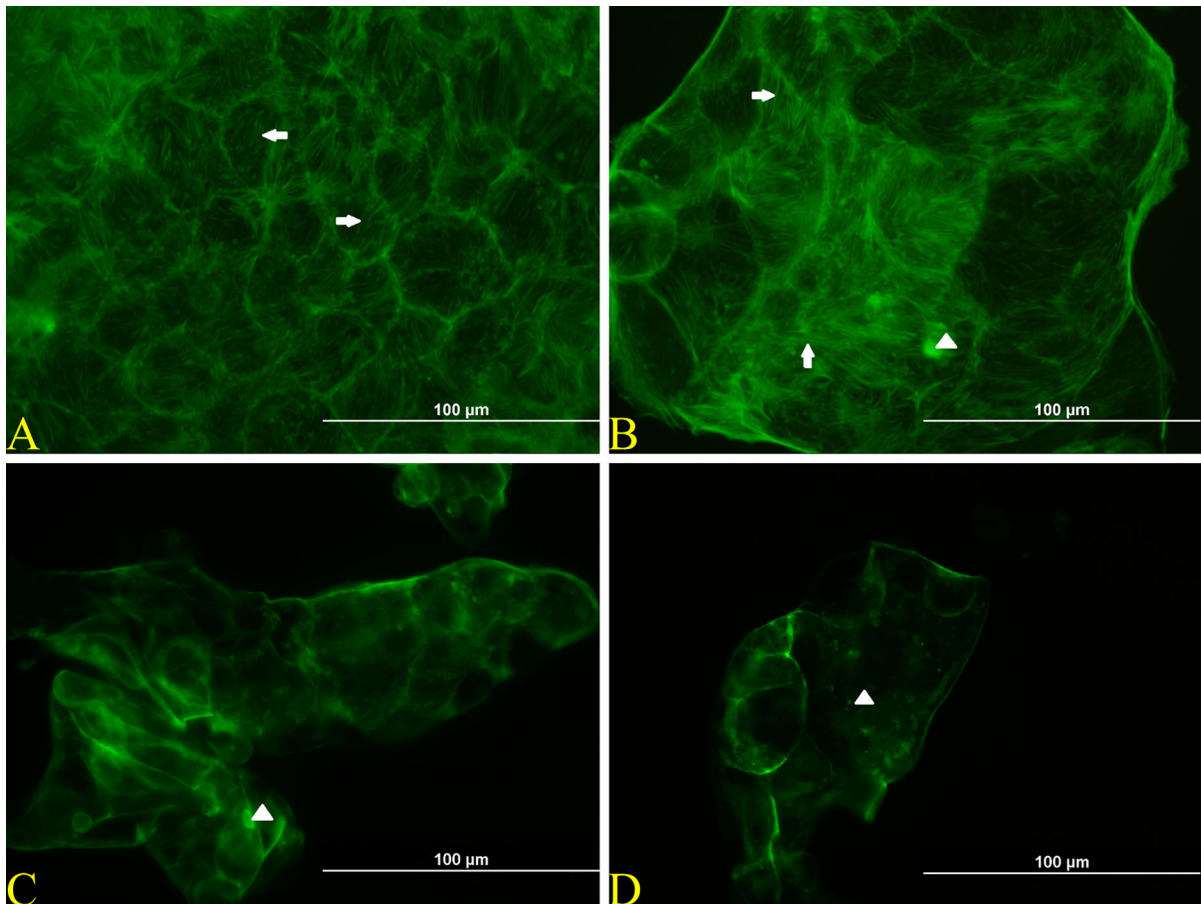

Fig. 15 Immunofluorescence staining of F-actin (*green*) in Caco-2 cells. The cells were untreated (**A**) or treated with HYP 0.04 μM (**B**), 0.08 μM (**C**) and 0.15 μM HYP (**D**), irradiated with 4 J/cm^2 and harvested 24 h after PDT. *arrow head* actin aggregates, *arrow* actin stress fibers. (Color figure online)
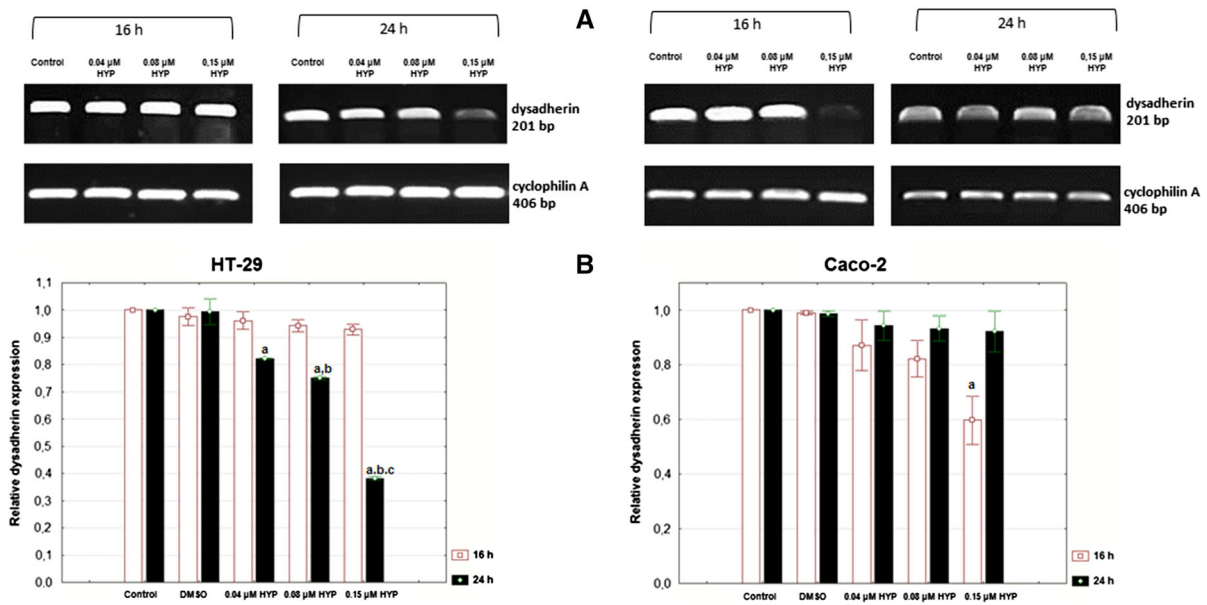
Fig. 16 **A** RT-PCR products of dysadherin and cyclophilin A isolated from HT-29 and Caco-2 cell lines. The 201 bp band for dysadherin and 406 bp band for cyclophilin A (positive control) were identified after seperation of products in 2 % agarose gel and stained wirth EtBr. **B** Relative dysadherin expression (dysadherin/cyclophilin A) according to measured intensities of bands. *a* Statistically significant from control group ($P \leq 0.001$), *b* statistically significant from 0.04 μM hypericin group, *c* statistically significant from 0.08 μM hypericin group ($P \leq 0.05$)


Fig. 17 Dysadherin expression was analysed by western blotting and densitometry in HT-29 cells 16 h and 24 h after PDT
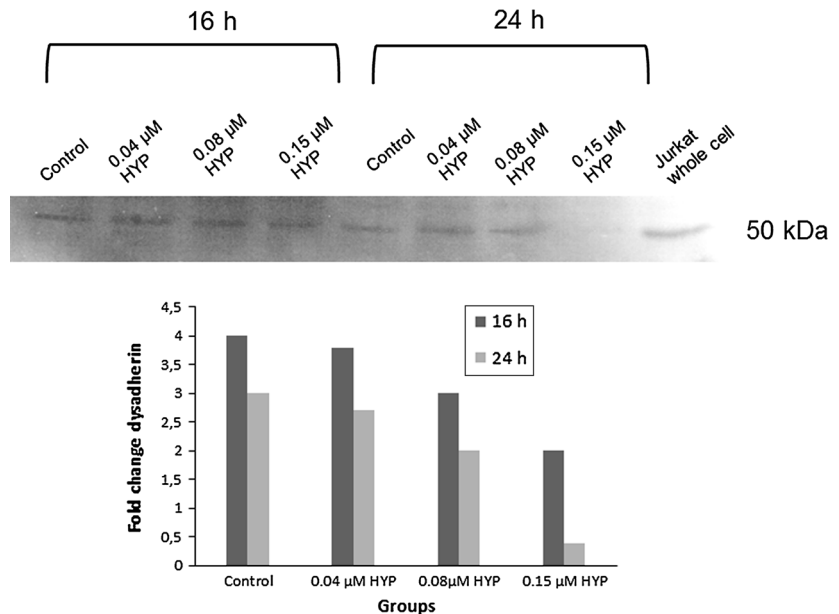
organisation, cell motility, focal adhesion in vitro and metastatic potential in vivo (Nam et al. 2007). Accordingly, in this study decline in dysadherin expression was parallel to decline in actin stress fibers, especially in the 0.08 and 0.15 μM HYP treatment groups. Blank et al. (2003) showed that HYP target heat shock protein 90 (HSP90) in tumor cells. HSP90 interacts with F-actin and stabilizes actin

Fig. 18 Dysadherin expression was analysed by western blotting and densitometry in Caco-2 cells 16 and 24 h after PDT
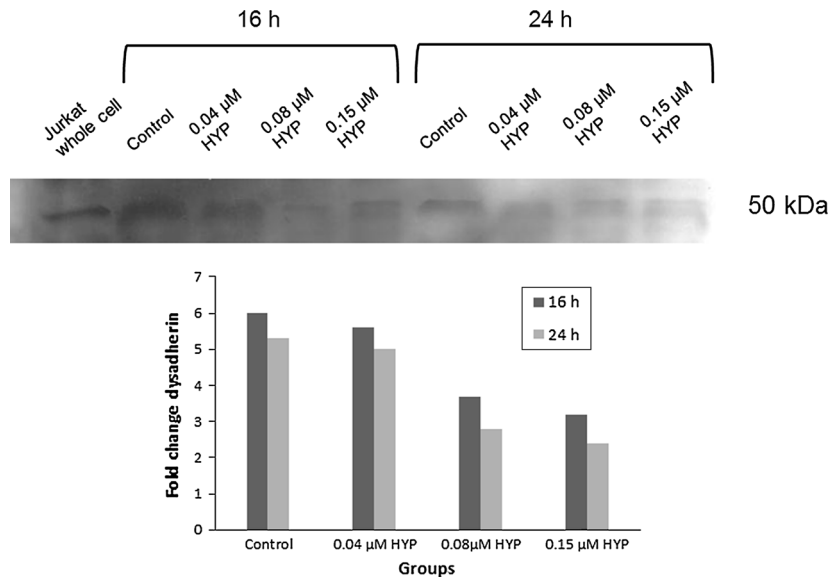
skeleton (Chaturvedi and Sreedhar 2010). Considering this, in our study, reorganisation of actin cytoskeleton after HYP-mediated PDT, could be related to the effect of HYP on HSP90 expression.

The reorganisation of microfilament network, especially the actin depolymerization has a significant role in the formation of apoptotic bodies in the early stages of apoptosis (Grzanka et al. 2003). In this study, increased apoptotic body formation was in parallel with decreased actin stress fibers and increased actin aggregate formation in the 0.08 and 0.15 μM HYP groups. In WiDr adenocarcinoma cells, aminolevulinic acid (ALA)-mediated PDT induced stress fibers. As a result of photoinhibition of cell detachment, the cell-substratum contacts strengthened and were governed by cellular signal transduction systems (Di Venosa et al. 2012). Similar to our results, after ALA-mediated PDT in HB4a cells, it was reported that F-actin disorganisation and damage were observed after ALA-mediated PDT in HB4a cells similar to our results.

Conclusion

This study shows that PDT results vary substantially with the cell type. After HYP-mediated PDT, HT-29 and Caco-2 colon adenocarcinoma cell lines responded distinctively. Additionally, it was shown that the type and the timing of cell death may alter.

0.08 μM HYP concentration induced the highest apoptosis and presented good PDT results after 24 h incubation for HT-29 cells and 16 h incubation for Caco-2 cells. We have demonstrated for the first time that there is an association between HYP-mediated PDT and decreased expression of dysadherin and reorganized F-actin in colon cancer cells.

References

Ackroyd R, Kelty C, Brown N, Reed M (2001) The history of photodetection and photodynamic therapy. Photochem Photobiol 74:656–669

Allison RR, Sibata CH (2010) Oncologic photodynamic therapy photosensitizers: a clinical review. Photodiagnosis Photodyn 7:61–75

Aoki S, Shimamura T, Shibata T, Nakanishi Y, Moriya Y, Sato Y, Kitajima M, Sakamoto M, Hirohashi S (2003) Prognostic significance of dysadherin expression in advanced colorectal carcinoma. Br J Cancer 88:726–732

Ashkenazi A (2002) Targeting death and decoy receptors of the tumour-necrosis factor superfamily. Nat Rev Drug Discov 2:420–430

Batistatou A, Charalabopoulos AK, Scopa CD, Nakanishi Y, Kappas A, Hirohashi S, Agnantis NJ, Charalabopoulos K (2006) Expression patterns of dysadherin and E-cadherin in

lymph node metastases of colorectal carcinoma. Virchows Arch 448:763–767

Blank M, Mandel M, Keisari Y, Meruelo D, Lavie G (2003) Enhanced ubiquitinylation of heat shock protein 90 as a potential mechanism for mitotic cell death in cancer cells induced with hypericin. Cancer Res 63:8241–8247

Buda A, Pignatelli M (2004) Cytoskeletal network in colon cancer: from genes to clinical application. Int J Biochem Cell Biol 36:759–765

Chaturvedi V, Sreedhar AS (2010) Hsp90 inhibition induces destabilization of actin cytoskeleton in tumor cells: Functional significance of Hsp90 interaction with F-actin. Asian Pac J Trop Med 3:715–722

Coates TD, Watts RG, Hartman R, Howard TH (1992) Distribution to development of polar shape in human polymorphonuclear neutrophils. J Cell Biol 117:765–774

Dahl JE, Mary J, Frangou-Polyzois MJ, Polyzois GL (2006) In vitro biocompatibility of denture relining materials. Gerodontology 23:17–22

Di Venosa G, Rodriguez L, Mamone L, Gándara L, Rossetti MV, Batlle A, Casas A (2012) Changes in actin and E-cadherin expression induced by 5-aminolevulinic acid photodynamic therapy in normal and ras-transfected human mammary cell lines. J Photochem Photobiol B Biol 106:47–52

Galanou MC, Theodossiou TA, Tsiourvas D, Sideratou Z, Paleos CM (2008) Interactive transport, subcellular relocation and enhanced phototoxicity of hypericin encapsulated in guanidinylated liposomes via molecular recognition. Photochem Photobiol 84:1073–1083

Grzanka A, Grzanka D, Orlikowska M (2003) Cytoskeletal reorganization during process of apoptosis induced by cytostatic drugs in K-562 and HL-60 leukemia cell lines. Biochem Pharmacol 66:1611–1617

Hendrickx N, Volanti C, Moens U, Seternes OM, de Witte P, Vandenheede JR, Piette J, Agostinis P (2003) Up-regulation of cyclooxygenase-2 and apoptosis resistance by p38 MAPK in hypericin-mediated photodynamic therapy of human cancer cells. J Biol Chem 278:52231–52239

Hirohashi S, Kanai Y (2003) Cell adhesion system and human cancer morphogenesis. Cancer Sci 94:575–581

Ino Y, Gotoh M, Sakamoto M, Tsukagoshi K, Hirohashi S (2002) Dysadherin a cancer associated cell membrane glycoprotein, down regulates E-cadherin and promotes metastasis. Med Sci 99:365–370

Jendzelovsky R, Mike J, Koval K, Soucek K, Procházková J, Kello M, Saková V, Hofmanová J, Kozubík A, Fedoroko P (2009) Drug efflux transporters, MRP1 and BCRP, affect the outcome of hypericin-mediated photodynamic therapy in HT-29 adenocarcinoma cells. Photochem Photobiol Sci 8:1716–1723

Kamuhabwa AR, Augustijns P, de Witte PA (1999) In vitro transport and uptake of protohypericin and hypericin in the Caco-2 model. Int J Pharm 188:81–86

Kaplan JH (2005) A moving new role for the sodium pump in epithelial cells and carcinomas. Sci STKE 289:31

Korb T, Schlüter K, Enns A, Spiegel HU, Senninger N, Nicolson GL, Haier J (2004) Integrity of actin fibers and microtubules influences metastatic tumor cell adhesion. Exp Cell Res 299:236–247

Ku GR, Tan LBH, Yau T, Boku N, Laohavinij S, Cheng AL, Kang YK, Lopes GL (2012) Management of colon cancer: resource-stratified guidelines from the Asian oncology. Lancet Oncol 13:e470–e481

Lev-Ari S, Strier L, Kazanov D, Shapiro LM, Sobol HD, Pinchuk I, Marian B, Lichtenberg D, Arber N (2005) Celecoxib and curcumin synergistically inhibit the growth of colorectal cancer cells. Clin Cancer Res 11:6738–6744

Mikeš J, Kleban J, Saèková V, Horváth V, Jamborová E, Vaculová A, Kozubík A, Hofmanová J, Fedoroèko P (2007) Necrosis predominates in the cell death of human colon adenocarcinoma HT-29 cells treated under variable conditions of photodynamic therapy with hypericin. Photochem Photobiol Sci 6:758–766

Mitchell DM, Ball JM (2004) Characterization of a spontaneously polarizing HT-29 cell line, HT-29/cl.f8. In Vitro Cell Dev Anim 40:297–301

Nam JS, Hirohashi S, Wakefield LM (2007) Dysadherin: a new player in cancer progression. Cancer Lett 255:161–169

Park JR, Kim RJ, Lee YK, Kim SR, Roh KJ, Oh SH, Kong G, Kang KS, Nam JS (2011) Dysadherin can enhance tumorigenesis by conferring properties of stem-like cells to hepatocellular carcinoma cells. J Hepatol 54:122–131

Paszkoa E, Ehrhardt C, Senge MO, Kelleher DP, Reynolds JV (2011) Nanodrug applications in photodynamic therapy. Photodiagnosis Photodyn 8:14–29

Ray RM, Bhattacharya S, Johnson LR (2011) Mdm2 inhibition induces apoptosis in p53 deficient humancolon cancer cells by activating p73-and E2F1mediatedexpression of PUMA and Siva-1. Apoptosis 16:35–44

Reed JC (1998) Bcl-2 family proteins. Oncogene 17:3225–3236

Salvador A (2008) Investigation about the mechanism of action of new antiproliferative compounds. Ph.D. thesis. Universita' Degli Studi Di Padova

Sanovic R, Verwanger T, Hartl A, Krammer B (2011) Low dose hypericin-PDT induces complete tumor regression in BALB/c mice bearing CT26 colon carcinoma. Photodiagnosis Photodyn Ther 8:291–296

Šemelakova M, Mikeš J, Jendzelovsky R, Fedorocko P (2012) The pro-apoptotic and anti-invasive effects of hypericin-mediated photodynamic therapy are enhanced by hyperforin or aristoforin in HT-29 colon adenocarcinoma cells. J Photochem Photobiol B Biol 117:115–125

Shimamura T, Yasuda J, Ino Y, Gotoh M, Tsuchiya A, Nakajima A, Sakamoto M, Kanai Y, Hirohashi S (2004) Dysadherin expression facilitates cell motility and metastatic potential of human pancreatic cancer cells. Cancer Res 64:6989–6995

Theodossiou TA, Hothersall JS, De Witte PA, Pantos A, Agostinis P (2009) The multifaceted photocytotoxic profile of hypericin. Mol Pharm 6:1775–1789

Wicki A, Lehembre F (2006) Tumor invasion in the absence of epithelialmesenchymal transition: podoplanin-mediated remodeling of the actin cytoskeleton. Cancer Cell 9:261–272

Yamazaki T, Yamazaki I, Nishimura Y, Dai R, Song PS (1993) Time-resolved fluorescence spectroscopy and photolysis of the photoreceptor blepharismin. Biochim Biophys Acta 1143:319–326

Yamazaki D, Kurisu S, Takenawa T (2005) Regulation of cancer cell motility through actin reorganization. Cancer Sci 96:379–386

Yang ZR, Liu M, Peng XL, Zhang JX, Dong WG (2012) Noscapine induces mitochondria-mediated apoptosis in human colon cancer cells in vivo and in vitro. Biochem Biophys Res Commun 421:627–633

Yoo JO, Ha KS (2012) New insights into the mechanisms for photodynamic therapy-induced cancer cell death. Int Rev Cel Mol Bio 295:139–174